Received: 8 October 2017 | Revised: 4 December 2017 | Accepted: 7 December 2017

DOI: 10.1002/er.3982

RESEARCH ARTICLE

WILEY INTERNATIONAL JOURNAL OF ENERGY RESEARCH

Enhanced radioluminescent nuclear battery by optimizing structural design of the phosphor layer

Zhiheng Xu[1] | Yunpeng Liu[1,2] | Zhengrong Zhang[1] | Wang Chen[1] | Zicheng Yuan[1] | Kai Liu[1] | Xiaobin Tang[1,2]

[1] Department of Nuclear Science and Engineering, Nanjing University of Aeronautics and Astronautics, Nanjing 211106, China

[2] Jiangsu Key Laboratory of Material and Technology for Energy Conversion, Nanjing 211106, China

Correspondence
Xiaobin Tang, Department of Nuclear Science and Engineering, Nanjing University of Aeronautics and Astronautics, Nanjing 211106, China.
Email: tangxiaobin@nuaa.edu.cn

Funding information
National Natural Science Foundation of China, Grant/Award Numbers: 11505096 and 11675076; Natural Science Foundation of Jiangsu Province, Grant/Award Number: BK20150735; Shanghai Aerospace Science and Technology Innovation Project, Grant/Award Number: SAST2016112; Funding of Jiangsu Innovation Program for Graduate Education, Grant/Award Number: KYLX15_0302; Priority Academic Program Development of Jiangsu Higher Education Institutions

Summary

Radioluminescent nuclear battery is a type of energy conversion device that can be miniaturized, which has the ability to convert nuclear energy into light energy, and again into electrical energy. To explore the response relationship between the phosphor layer structure and the electrical performance of radioluminescent nuclear battery, the physical model was established to research the deposition energy distribution by using Monte Carlo method. The radioluminescence spectra and current-voltage characteristic curves were used to investigate the optical and electrical properties. Through a comprehensive comparison of single plane layer, double plane layer, and V groove layer structures, the simulated results are consistent with experimental results. The results indicate that the Monte Carlo simulation is applicable to analysis of the phosphor layer structure of radioluminescent nuclear battery. Additionally, the results also show that the structure type and physical parameters of the phosphor layer have great influence on the energy deposition. A suitable phosphor layer structure can provide a new route to exhibit higher energy conversion efficiency as well as improving the matching degree between the range of radioactive particles and the thickness of the phosphor layer.

KEYWORDS

energy conversion, Monte Carlo simulation, radioluminescent nuclear battery, structure optimization, β source

1 | INTRODUCTION

Radioluminescent nuclear battery is proposed and developed on the basis of more mature and thorough study of betavoltaic nuclear battery techniques.[1-3] The main difference between the 2 types of batteries is that the former adds an intermediate energy conversion process, while the integrated battery structure adds a phosphor layer. So the whole energy conversion process of radioluminescent nuclear battery is from nuclear energy to light energy, and then again to electric energy.[4-6] It works because phosphor layers can emit visible light under radioactive particles excitation, and the light is powerful enough to knock electrons free from atoms. The electrons go on to form a useful direct current by photovoltaic devices. Numerous scientific researchers have aimed to establish a nuclear power supply system with long life, high energy density and strong adaptability.[7-9] However, due to the low level of energy conversion efficiency of the radioluminescent nuclear battery at this stage, its promotion and application are severely limited.

Through the development of radioluminescent nuclear battery over several decades, the research works mainly focus on revealing the influence factors of battery and improving the performance of electrical output. Specific research contents include changing experimental materials, varying physical parameters, optimizing structural design, and analyzing environmental factors.[10-14] According to previous research results, it was found that selecting the excellent performance materials, proper coupling between these materials, and optimizing the battery structure are required to achieve maximum nuclear-to-electrical conversion efficiency.[15,16] Meanwhile, in view of the indirect energy conversion mechanism of this nuclear battery, the phosphor layer is an intermediate energy transducer. On the one hand, the phosphor layer absorbs radiation particles bombarding, undergoes radiative excitation, and releases luminescent photons of a specific wavelength range. On the other hand, it also holds the task of photons emission and transmission.[17] Therefore, optimizing the structure of the phosphor layer is an important breakthrough to realize the improvement of battery performance, especially in the case of the 3 main materials, and their physical parameters have been determined.

The purpose of this study is presenting the internal response relationship between the phosphor layer structure and the performance parameters, such as the luminescent intensity and the maximum output power of radioluminescent nuclear battery. Furthermore, experimental details of ZnS:Cu phosphor layer radioluminescence (RL) and its application in the nuclear battery with planar β sources of different energies are stated. The phosphor layers are prepared into single plane, double plane, and V groove structures. Monte Carlo N-Particle Transport Code version 5 simulation was performed to examine beta particles depositions on different ZnS:Cu phosphor layers. The influence of phosphor powder concentration and phosphor layer geometry on deposition energy, RL intensity, and electrical output of batteries was studied.

2 | MATERIALS AND METHODS

There are 3 physical simulation models of single plane, double plane, and V groove ZnS:Cu phosphor layers, as shown in Figure 1. The phosphor layer contains 2 parts: radioluminescent ZnS:Cu phosphors as transducer and transparent adhesion layer as substrate, and their thickness is 16 and 29 μm, respectively. Single plane layers are designed as positive and negative 2 structures as shown in Figure 1A, of which the positive structure refers to the ZnS:Cu phosphors toward the radioactive source and the negative structure means the adhesion layer toward the radioactive source. Similarly, double plane layers have positive-positive, positive-negative, negative-positive, and negative-negative 4 structural designs as shown in Figure 1B. The meaning of positive and negative is the same as that for the single plane layer. The initial size of the phosphor layers is 3 cm × 3 cm, where the V groove phosphor layer is folded on the basis of the initial phosphor layer along the center line. V groove phosphor layers are designed in 2 forms of 2V and 4V groove. The bending angle is all 90° as shown in Figure 1C, and their projection area is 2.12 cm × 3 cm.

Two beta sources of different particle energies, ^{63}Ni and ^{147}Pm, were used as the excitation source of the nuclear battery, respectively. In the Monte Carlo N-Particle Transport Code simulation, the 2 sources are set to round thin sheet with a radius of 1.5 cm, and the continuous beta energy spectra is used in the calculation model. The surface of the phosphor layer corresponding

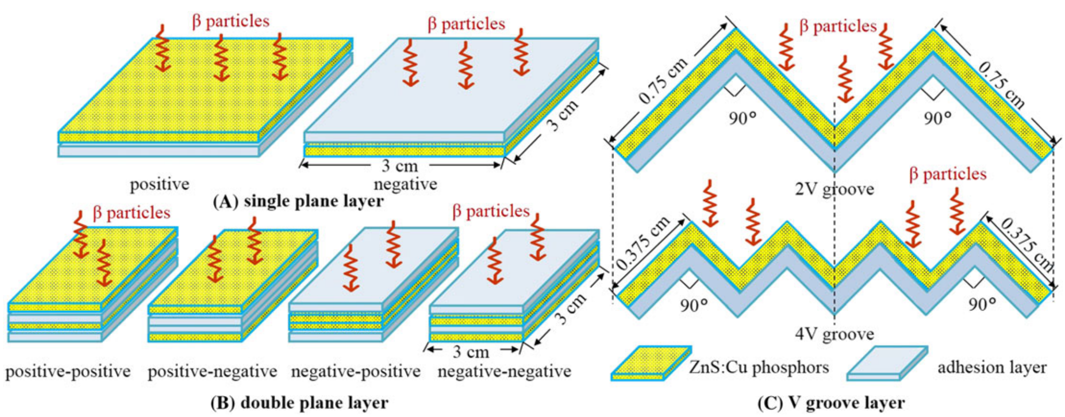

FIGURE 1 The physical model for the Monte Carlo N-Particle Transport Code simulation [Colour figure can be viewed at wileyonlinelibrary.com]

to the beta source is identified as the incident plane, and its distance from the plane source is infinitely close to zero (set it to 1E-10 cm in the simulation).

Radioluminescence spectra of the ZnS:Cu phosphor layers under different beta particle excitation sources were performed by a Cary Eclipse fluorescence spectrophotometer (Agilent Technologies, USA). The phosphor layers have 3 types of structures mentioned above, and beta sources are 4.93 mCi/cm^2 ^{63}Ni and 2.88 mCi/cm^2 ^{147}Pm. The radioluminescent nuclear battery experimental apparatus consisted of ZnS:Cu phosphor layer, GaAs single-junction photovoltaic device, and a beta source, as shown in Figure 2. During the experiment, the phosphor layer and beta source, in turn, were selected and assembled into the nuclear battery. The current-voltage (*I-V*) characteristics of the battery were measured by a dual-channel system source-meter instrument (Model 2636A, Keithley, USA). In all RL and *I-V* measurements, the samples were shielded from light and electromagnetic interference and tested at room temperature around 298 K and 1 atmospheric pressure.

3 | RESULTS AND DISCUSSION

3.1 | Monte Carlo simulation

The results of the radiation particles deposited on the phosphor layers with various combinations are provided in Table 1. The percentage is the ratio between the deposition energy of the beta particles in the phosphor layer and the source initial energy in the energy conversion process. The number of simulated particles was 3 × 10^8, and the errors were all less than 0.05%. Figure 3 shows the accumulated beta energy distribution in the ZnS:Cu plane phosphor layer. The simulation results reflect that for ^{63}Ni and ^{147}Pm beta sources, the particle transmission track depth in the phosphor layer is about 10.4 to 16 μm and 70 to 123 μm, respectively. Due to the different range of the released beta particles, the single plane phosphor layer is almost enough for the ^{63}Ni source, so the radiation deposition energy of the double plane phosphor layer is almost the same as the single layer; but for the ^{147}Pm source, the deposition energy of the double plane phosphor layer is significantly larger than the single. Whether for the ^{63}Ni or ^{147}Pm source, the arrangement of the first layer of the plane phosphor layer is crucial and it plays a decisive role from the results of comparison. When the structure type of the phosphor layer is V groove, the radiant deposition energy in the phosphor of 4V groove structure is significantly higher than that of the 2V structure. This is primarily due to the difference in height between these 2 structures, although their bottom projection area is the same. The structure of the phosphor layer not only changes the content of the irradiated phosphor per unit area but also affects the distance between the beta source and the phosphor layer. Therefore, the combination of the different physical parameters of the radioactive source and the phosphor layer will produce different consequences. For the ^{63}Ni source with lower beta particle energy and shorter average range, the structural effect of the phosphor layer on the deposition energy is greater.

3.2 | RL spectra and *I-V* characteristic curves

Figure 4 contains the RL spectra of the ZnS:Cu single plane phosphor layer under the mentioned ^{63}Ni or ^{147}Pm beta source and the corresponding *I-V* characteristics of the combinatorial nuclear battery. The luminescence intensity of the phosphor layer with different monolayer structure is altered under the same excitation condition, as well as the electrical output parameters. However, no matter what kind of β source excitation, the RL spectra of the different phosphor layers are similar, and the peak wavelengths of the emission

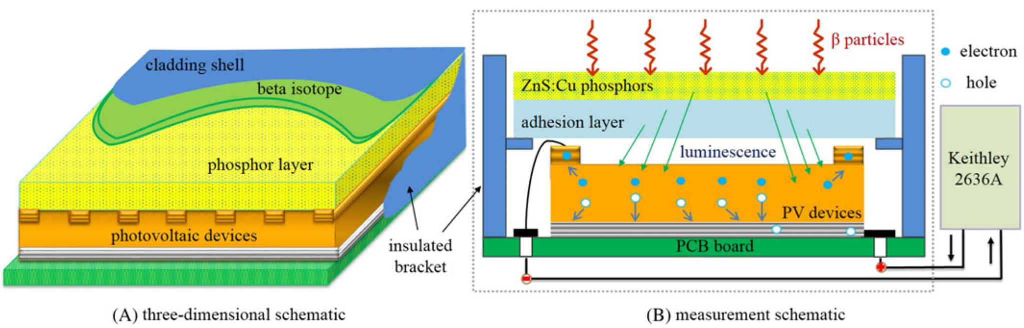

FIGURE 2 The 3-dimensional and measurement schematic of beta radioluminescent nuclear battery. PCB, printed circuit board [Colour figure can be viewed at wileyonlinelibrary.com]

TABLE 1 Radiation energy deposition percentage of different phosphor layers (the "+" means a little bit bigger than that)

Structure Type	Energy Deposition Percentage, %		Structure Type	Energy Deposition Percentage, %	
	^{63}Ni	^{147}Pm		^{63}Ni	^{147}Pm
Positive	59.84	42.97	Positive-positive	59.84	49.98
Negative	0.93	20.59	Positive-negative	59.84+	47.39
2V groove	46.02	52.64	Negative-positive	0.93	27.95
4V groove	59.85	63.07	Negative-negative	0.93+	24.97

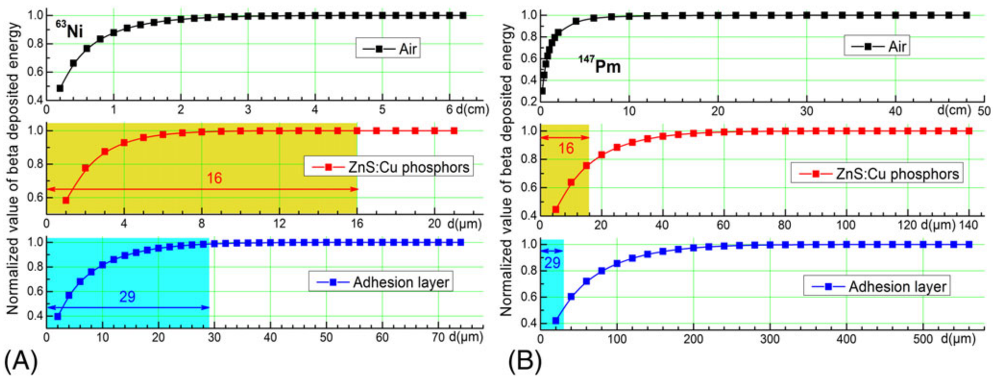

FIGURE 3 Relationship between beta energy deposition and material thickness. A, ^{63}Ni source. B, ^{147}Pm source [Colour figure can be viewed at wileyonlinelibrary.com]

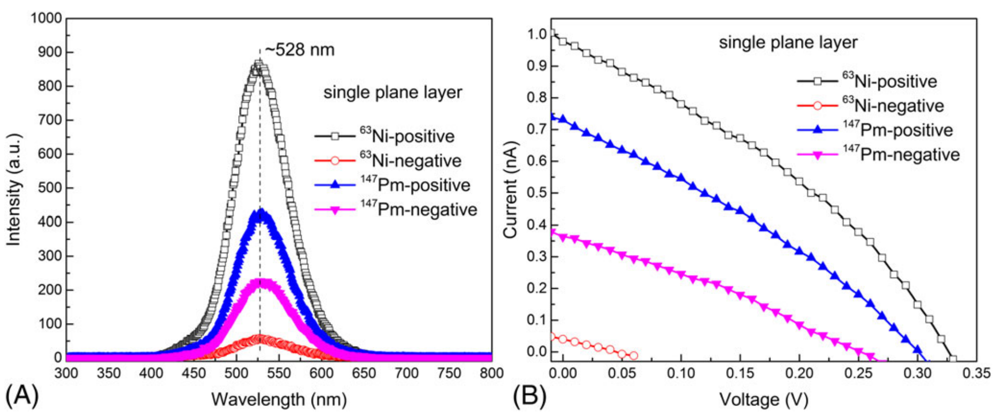

FIGURE 4 A, Radioluminescence spectra and B, current-voltage characteristic curves of single plane phosphor layer under different beta sources [Colour figure can be viewed at wileyonlinelibrary.com]

spectra are about 528 nm. Since GaAs photovoltaic device used in each combination nuclear battery is the same one, the internal relationship between the output power and the luminescence intensity can be reversed according to the final electrical test results. Comparison of the optical and electrical performance test results can be found that the optimal and worst order of different combinations is consistent. The single positive structure is obviously superior to the single negative structure, which is corresponding with the simulation results. According to Monte Carlo simulation results, the track depth and the deposition behavior of the 2 different beta sources in the phosphor layer are different. The penetration depth of ^{147}Pm source is much larger than the ^{63}Ni source. In addition, the thickness of ZnS:Cu phosphors is 16 μm, which is close to the penetration depth of ^{63}Ni source. At the same time, the difference in activity density makes the number of particles released from the source surface per unit time different. Due to the deposition of beta particles and the activity of radioactive sources, so that the output performance of battery using ^{63}Ni is better than that using ^{147}Pm with the same positive single plane phosphor layer structure.

The RL spectra and the corresponding *I-V* characteristics for the ZnS:Cu double plane phosphor layer are tested and shown in Figure 5. For both ^{63}Ni and ^{147}Pm sources, when the first layer of the double plane phosphor layer structure is positive, the optical and electrical properties always better than those of the first layer are negative. The effect of the positive and negative forms of the first layer of the phosphor layer on the output performance is significant. The transparent adhesion layer has the effect of blocking, absorbing and attenuating the kinetic energy of β particles, and the phosphor has self-absorption effect on the luminescence, which reduce the luminescence intensity of the phosphor layer. In contrast, the energy loss of luminescence in the adhesion layer is significantly lower than that of beta particles. Therefore, in the case where the phosphor layer faces the radiation source, that is, when the phosphor layer structure is positive, absorption of the incident radiation and transmission of the emitted luminescence are more favorable, and the overall energy conversion of the nuclear battery is more efficient. For the beta source with a lower particle emission energy, this is even more so.

The effect of the second phosphor layer depends on the range of the β particles. Since the phosphor's thickness of the first layer is similar to that of the particles' range, the enhancement of the second phosphor layer is not obvious for ^{63}Ni source and even causes the opposite effect. There is also an interesting phenomenon, which is that when the second layer is negative form, the performance is relatively better. This may also confirm that the light absorption effect of the adhesion layer is weaker than that of the phosphors. However, for the ^{147}Pm source with a longer particle range, the second phosphor layer can bring significant improvement effect. It can also be found that the performance is better when the second phosphor layer is positive. The experimental results also show that the RL effect of the phosphors in the second phosphor layer is stronger than that of the light self-absorption effect.

Figure 6 shows the RL spectra and the corresponding *I-V* characteristics of V-groove phosphor layer under different beta sources. Although the bottom projection area and the phosphor content are identical for the 2V and 4V groove, the 4V groove structure shortens the distance between the radiation source and the phosphor layer by half, resulting in less energy loss. Therefore, under excitation by ^{63}Ni or ^{147}Pm source, the 4V groove has always a better performance than 2V groove, which is also consistent with the Monte Carlo simulation results. It was found that when the phosphor layer changed from 2V to 4V, under ^{63}Ni and ^{147}Pm sources, the final maximum output power increased by 75.2% and 26.61%, respectively.

3.3 | Performance comparison of different phosphor layer structures

Although both the plane structure and V groove structure are single-layer phosphor layer, their performance is very different. For the ^{147}Pm source, the performance of the V-shaped phosphor layer structure is significantly better than the plane structure. This is mainly due to the fact that the structure of the phosphor layer not only changes the deposition energy in the phosphors but also affects the transmission, transport, and absorption of luminescent photons.[18,19] As a whole, the activity of the radioactive source, the range of beta particles, the luminous flux, and the effective working area also have an impact on the performance of the nuclear battery. According to the Monte Carlo calculation results, the deposition behavior of beta particles in each phosphor layer structure can be analyzed. Through the experimental tested spectra, the

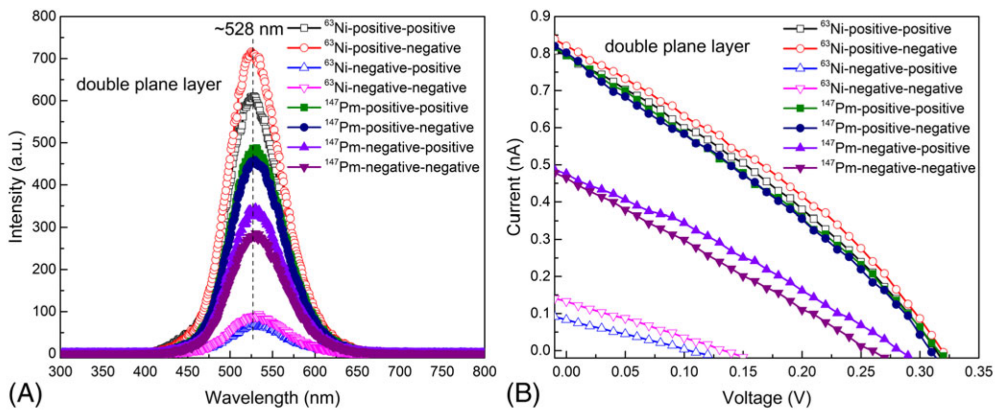

FIGURE 5 A, Radioluminescence spectra and B, current-voltage characteristic curves of double plane phosphor layer under different beta sources [Colour figure can be viewed at wileyonlinelibrary.com]

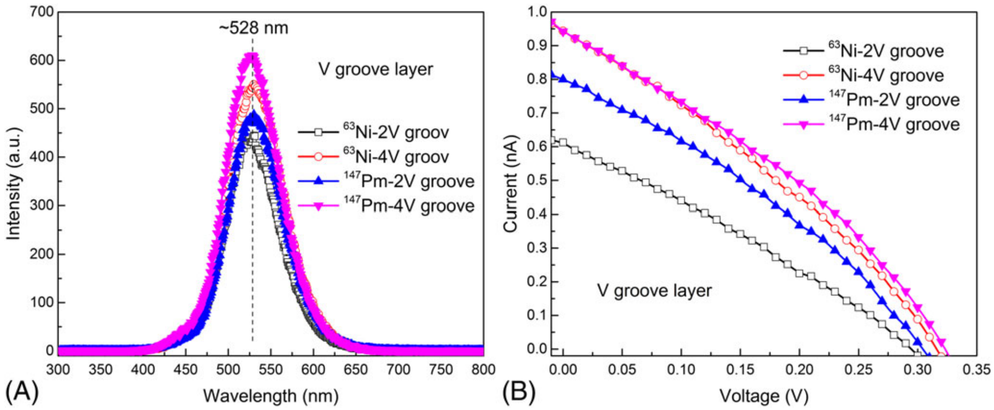

FIGURE 6 A, Radioluminescence spectra and B, current-voltage characteristic curves of V groove phosphor layer under different beta sources [Colour figure can be viewed at wileyonlinelibrary.com]

emission intensity of different phosphor layer structures can be obtained. The two processes of radioluminescence and photovoltaic in radioluminescent nuclear batteries are continuous and simultaneous. On the one hand, the V groove structure can effectively increase the phosphor powder content in unit area, and improve the luminescence intensity. But on the other hand, it also increases the distance between the radioactive source and the phosphor layer, and creates a larger air blocking effect. Therefore, the final electrical output performance is the product of a comprehensive trade-off.

Figure 7 shows the radiation energy deposition, optical performance, and electrical performance of different conditions. For the "Ni-P" with similar particle range and phosphors thickness, the performance in all aspects performed better. The maximum power per unit area of the battery with "Ni-P" reaches 0.1075 nW/cm^2. When the particle has a larger range than the thickness of ZnS: Cu phosphors, 4V groove structure exhibits an obvious advantage. As shown in Figure 7, the maximum power

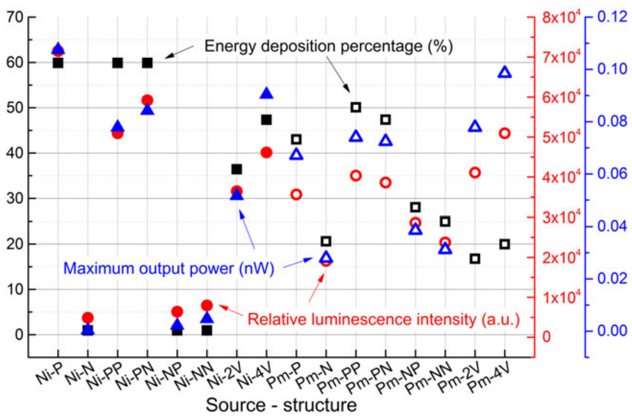

FIGURE 7 Performance comparison of beta energy deposition percentage, radioluminescent intensity, and the maximum output power for the phosphor layers with different geometric structures [Colour figure can be viewed at wileyonlinelibrary.com]

per unit area of the battery has been obtained as 0.0985 nW/cm^2 for the "Pm-4V" in comparison with 0.0671 nW/cm^2 for the "Pm-P". At the same time, the variation trends of beta energy deposition percentage in phosphors, RL intensity, and the maximum output power with different geometric structures of the phosphor layers are similar. A good match between the experimental and calculation results also validates the correctness of the theoretical discussion. These curves with similar variations also reflect that the optical and electrical output properties can be roughly learned by analyzing their deposition energy, in the case of the same photovoltaic device and unchanged test temperature.

The overall energy conversion efficiency η represents the ratio of the available electrical power output P_{out} from the photovoltaic device, compared to the decay energy P_{in} of the used radiation source, which is calculated by the following Equations 1 and 2.[20,21]

$$\eta = \frac{P_{out}}{P_{in}} = \frac{P_{max}}{AE_{\beta}} \times 100\%, \tag{1}$$

$$P_{max} = \max(I \times V), \tag{2}$$

where the maximum power P_{max} is the maximum value obtained by the product of the current and the voltage, which can be easily calculated along the *I-V* sweep. P_{out} can be taken to be P_{max} since the battery can be operated up to its maximum power output to get the maximum efficiency. A and E_{β} are the activity and the average energy of the beta source, respectively. Figure 8 compares the overall energy conversion efficiency when different structured phosphor layers were applied to the radioluminescent nuclear battery. For the lower energy of ^{63}Ni beta source, the difference between the different structural schemes is very obvious. When the thickness of the phosphors

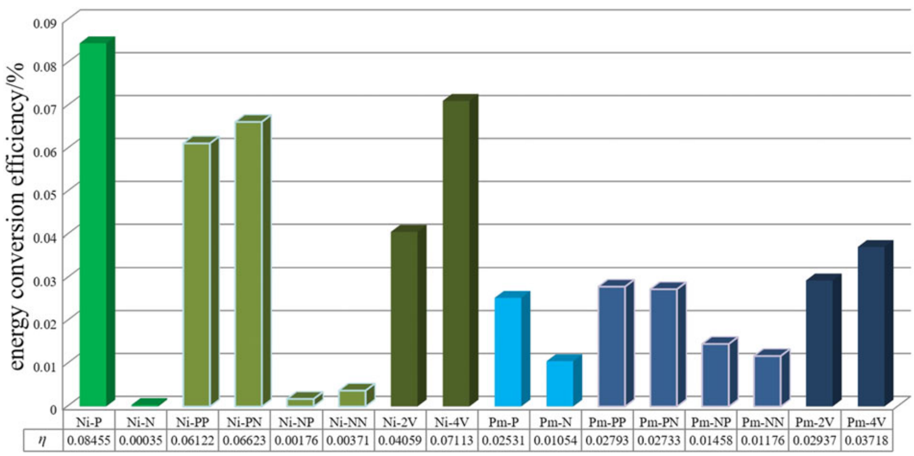

FIGURE 8 The energy conversion efficiency of the battery with different phosphor layers [Colour figure can be viewed at wileyonlinelibrary.com]

matches the particle range of the ^{63}Ni source, the single phosphor layer combination (Ni-P) can present a good result. For the ^{147}Pm beta source, the V groove structure can indeed improve the output performance to a certain extent. A maximum energy conversion efficiency of approximately 0.085% was obtained for "Ni-P" with a phosphor thickness of 16 μm and an activity density of 4.93 mCi/cm^2. When the structure is converted from "Pm-P" to "Pm-4V", the overall energy conversion efficiency was increased by nearly 1.5 times. The results have been borne out again that there is a matching optimization problem between the particle range of the source and the structural parameters of the phosphor layer. Comparing all the combinations, it also can be speculated that improving the matching degree of the battery materials can effectively increase the energy conversion efficiency.

3.4 | Optimization simulation of the V groove layer

The simulation results are in good agreement with the experimental results, indicating that the Monte Carlo method can be used to the optimization design of the phosphor layer structure in radioluminescent nuclear battery. The influence of the structural parameters, such as the intersection angle θ and the height of the V groove phosphor layer H, on the deposition energy of the β particles in the phosphor layer was further explored. In the simulation model, the outer diameter of both ^{63}Ni and ^{147}Pm unidirectional surface sources was set to 2.5 cm, and the projection area of the phosphor layers was fixed at 3 cm × 3 cm. The center of the source and the phosphor layers was aligned, and the other conditions were consistent with the previous simulation parameters. The aim is to eliminate the edge effect of β particles and phosphors.

The beta particle energy deposition analysis shown in Figure 9 revealed that the track behavior of the particles in the material is obviously affected by the angle and height of the V groove structured phosphor layer fluorescent layer. It can be noted that there is an optimal value of

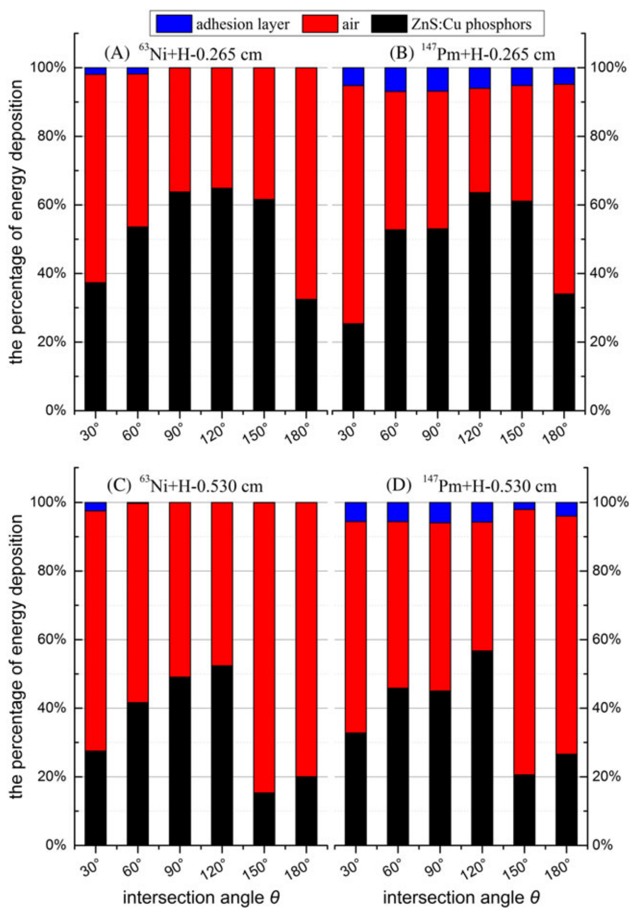

FIGURE 9 Relationship between the percentage of energy deposition and structural parameter of V groove phosphor layer [Colour figure can be viewed at wileyonlinelibrary.com]

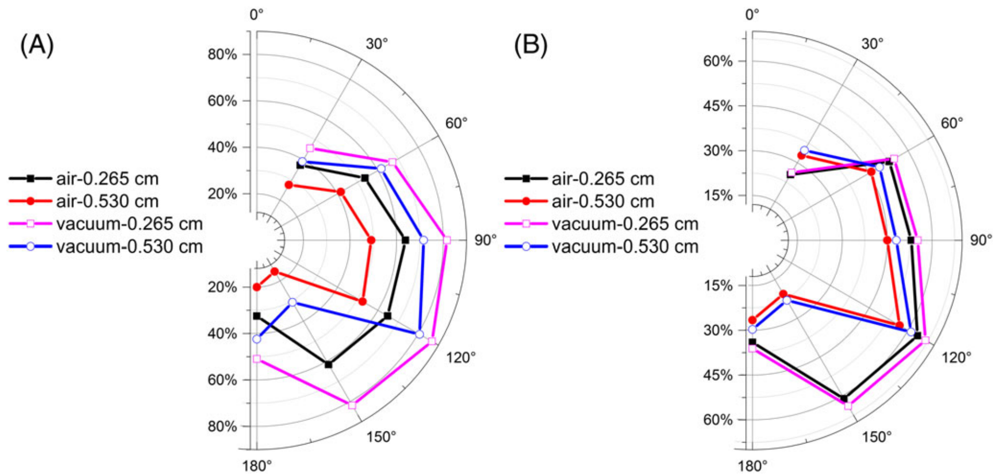

FIGURE 10 The energy deposition percentage of V groove phosphor layer in air and vacuum environment. A, ^{63}Ni source. B, ^{147}Pm source [Colour figure can be viewed at wileyonlinelibrary.com]

the angle to maximize the energy deposition rate in the phosphors. In general, for the same excitation source and angle, the lower the height of the phosphor layer in a certain range, the higher the percentage of energy deposition in the phosphors. For the uniform height of the phosphor layer, the variation tendency of the percentage with angle is similar, under the excitation of different sources. Due to the ^{147}Pm with a higher average energy, the percentage of energy deposition in the adhesion layer is also larger.

The energy deposited in the air occupies a comparatively big share according to the obtained data. Due to the air barrier effect, the air gap between the beta source and the phosphor layer affects the transport of luminescent photons, which also cause the loss of radiation energy. Therefore, the vacuum environment is more favorable for the deposition of β particles in the phosphors; the increase in the percentage of energy deposition will be more significant, especially for the low-energy radiation particles. Figure 10 shows the variation of the percentage of energy deposition in the phosphors with the structural parameters of the V groove phosphor layer under the conditions of air and vacuum. For the constant excitation source and phosphor layer, the trend of energy deposition percentage in the phosphors change with intersection angle in vacuum is similar to that in air environment. It is also interesting to find that in both environments, when the intersection angle is 120°, the energy deposition percentage in the phosphors is the largest regardless of the height H. This may be the product of a trade-off between the phosphor contents, the air resistance, and other factors.

As the height of the phosphor layer is 5 cm and the intersection angle is 30°, the percentage of energy deposition in the phosphors increases by 99.83% and 11.78% respectively under the excitation of ^{63}Ni and ^{147}Pm sources when the air environment becomes a vacuum. It means that using phosphor layer structure optimization design and vacuum packaging to improve the output performance of radioluminescent nuclear battery is an effective reference for future battery designers.

4 | CONCLUSION

This article began with a brief analysis about the developing tendency of radioluminescent nuclear battery. The main study focus on how phosphor layer structure influences the energy deposition of the beta particles in the phosphors and the luminescence intensity, which are directly related to the output power and efficiency of the battery. The energy deposition of beta particles in the different structural phosphor layers calculated from the simulation shows that there is an efficient coupling between the range of the particle and the thickness of the phosphors. It is confirmed that the emission wavelength of the phosphor layer is not affected by the structure parameters. On the other hand, the structure of the phosphor layers can be used to adjust the process of energy deposition and luminescent transport, which are positively correlated with the electrical output performance of the radioluminescent nuclear batteries.

Based on the simulation and experimental results, it also can be seen that the Monte Carlo method is feasible to optimize the structural design of the phosphor layer and evaluate the electrical performance of the battery. In addition, the radiation energy deposition in the phosphors can be enhanced by optimizing the structure type and physical parameters of the phosphor layer and placing the battery in a vacuum environment. These measures confirm that the transport behavior of luminescent photons in the material can be effectively improved, thus reducing the energy dissipation and realizing the enhancement of the luminescence intensity of the phosphor layer and the energy conversion efficiency of the battery.

ACKNOWLEDGEMENTS

This work was financially supported by the National Natural Science Foundation of China (grant nos. 11675076 and 11505096), the Natural Science Foundation of Jiangsu Province (BK20150735), the Shanghai Aerospace Science and Technology Innovation Project (grant no. SAST2016112), the Funding of Jiangsu Innovation Program for Graduate Education (grant no. KYLX15_0302), and the Priority Academic Program Development of Jiangsu Higher Education Institutions.

ORCID

Zhiheng Xu http://orcid.org/0000-0002-9229-8558
Xiaobin Tang http://orcid.org/0000-0003-3308-0468

REFERENCES

1. Liu YP, Tang XB, Xu ZH, Hong L, Wang P, Chen D. Optimization and temperature effects on sandwich betavoltaic microbattery. *Sci China Technol Sci*. 2014;57(1):14-18.
2. San H, Yao S, Wang X, Cheng Z, Chen X. Design and simulation of GaN based Schottky betavoltaic nuclear micro-battery. *Appl Radiat Isot*. 2013;80:17-22.
3. Bower KE, Barbanel YA, Shreter YG, Bohnert GW. *Polymers, Phosphors, and Voltaics for Radioisotope Microbatteries*. Boca Raton: CRC press; 2002:35-51.
4. Landis GA, Bailey SG, Clark EB, Myers MG, Piszczor MF, Murbach MS. Non-solar photovoltaics for small space missions. In: *2012 38th IEEE Photovoltaic Specialists Conference (PVSC)*, Austin, TX; 2012: 002819–002824.
5. Prelas MA, Weaver CL, Watermann ML, Schott RJ, Wisniewski DA. A review of nuclear batteries. *Prog Nucl Energy*. 2014;75:117-148.
6. Sychov M, Kavetsky A, Yakubova G, et al. Alpha indirect conversion radioisotope power source. *Appl Radiat Isot*. 2008;66(2):173-177.
7. Schmidt G, Dudzinski L, Sutliff T. Radioisotope power: a key technology for deep space exploration. In: *6th International Energy Conversion Engineering Conference (IECEC)*, Cleveland, Ohio; 2011: 5640.
8. Walton R, Anthony C, Ward M, Metje N, Chapman DN. Radioisotopic battery and capacitor system for powering wireless sensor networks. *Sensors Actuators A Phys*. 2013;203:405-412.
9. Cress CD, Redino CS, Landi BJ, Raffaelle RP. Alpha-particle-induced luminescence of rare-earth-doped Y_2O_3 nanophosphors. *J Solid State Chem*. 2008;181(8):2041-2045.
10. Sharma A, Melancon J, Bailey S, Zivanovic S. Novel use of semiconductive conjugated polymer with optimized scintillator for betavoltaic applications. In: *ASME 2015 International Mechanical Engineering Congress and Exposition*, American Society of Mechanical Engineers; 2015: V06BT07A041.
11. Lee H, Yim MS. Examination of scintillator-photovoltaic cell-based spent fuel radiation energy conversion for electricity generation. *Prog Nucl Energy*. 2017;94:46-54.
12. Hong L, Tang XB, Xu ZH, Liu YP, Chen D. Radioluminescent nuclear batteries with different phosphor layers. *Nucl Instrum Methods Phys Res, Sect B*. 2014;338:112-118.
13. Tang XB, Hong L, Xu ZH, Liu YP, Chen D. Temperature effect of a radioluminescent nuclear battery based on ^{147}Pm/ZnS: Cu/GaAs. *Appl Radiat Isot*. 2015;97:118-124.
14. Russo J, Litz M, Ray W, Smith B, Moyers R. A radioluminescent nuclear battery using volumetric configuration: ^{63}Ni solution/ZnS: Cu, Al/InGaP. *Appl Radiat Isot*. 2017. https://doi.org/10.1016/j.apradiso.2017.09.018
15. Kim T, Lee N, Jung HK, Kim JH. Enhancement of energy performance in betavoltaic cells by optimizing self-absorption of beta particles. *Int J Energy Res*. 2016;40(4):522-528.
16. Yürük RK, Tütüncüler H. Investigation of the effect of beta source and phosphors on photovoltaic cells. In: *AIP Conference Proceedings*. AIP Publishing, 2017;1815(1):040002.
17. Xu ZH, Tang XB, Hong L, Liu YP, Chen D. Structural effects of ZnS:Cu phosphor layers on beta radioluminescence nuclear battery. *J Radioanal Nucl Chem*. 2015;303(3):2313-2320.
18. Yu RY, Jin SZ, Cen SY, Liang P. Effect of the phosphor geometry on the luminous flux of phosphor-converted light-emitting diodes. *IEEE Photon Technol Lett*. 2010;22(23):1765-1767.
19. Theirrattanakul S, Prelas M. A methodology for efficiency optimization of betavoltaic cell design using an isotropic planar source having an energy dependent beta particle distribution. *Appl Radiat Isot*. 2017;127:41-46.
20. Xu ZH, Tang XB, Hong L, Liu YP, Chen D. Development of a beta radioluminescence nuclear battery. *Nucl Sci Tech*. 2014;25(4):040603
21. Hong L, Tang XB, Xu ZH, Liu YP, Chen D. Parameter optimization and experiment verification for a beta radioluminescence nuclear battery. *J Radioanal Nucl Chem*. 2014;302(1):701-707.

How to cite this article: Xu Z, Liu Y, Zhang Z, et al. Enhanced radioluminescent nuclear battery by optimizing structural design of the phosphor layer. *Int J Energy Res*. 2018;42:1729–1737. https://doi.org/10.1002/er.3982